

Non-isolated high voltage gain DC to DC converter based on the diode a capacitor switches

Ibraheem Jawad Billy, Jasim Farhood Hussein

Department of Electrical Engineering, College of Engineering, Technology University, Baghdad, Iraq

Article Info

Article history:

Received Feb 8, 2022

Revised Jul 1, 2022

Accepted Jul 15, 2022

Keywords:

Current-ripple

DC to DC converter

Multi-phase boost converter

Switches voltage stress

Voltage multiplier

ABSTRACT

Many researchers have put great endeavor to develop DC converter's designs, into studying how to increase voltage gain with low switching stress and low ripple current. This paper has proposed a circuit to boost the voltage with a high gain conversion ratio. It is a combined adverse parallel two boost conversion. Two inductors are connected on both sides of the input source to decrease the current-ripple of the input current and output sides utilizing the interleaving technique. The proposed converter integrated with an active-network circuit is based on multiplier cells and two output capacitors. The voltage gain and voltage stresses across power semiconductors have been determined using a steady-state analysis. In addition, the input current-ripple and output voltage-ripple are analysis have been reported. This converter's inductors operate in a continuous conduction mode (CCM). The designed converter is capable of achieving significant voltage gain while maintaining a low duty ratio. Furthermore, the active switches and output diodes are under low voltage stress. As a result, low voltage components can be used to decrease conduction loss and cost. Finally, this converter was simulated in MATLAB/Simulink software to verify the theoretical calculations.

This is an open access article under the [CC BY-SA](https://creativecommons.org/licenses/by-sa/4.0/) license.



Corresponding Author:

Ibraheem Jawad Billy

College of Engineering, Technology University

Industry Street, Baghdad, Iraq

Email: eee.20.28@grad.uotechnology.edu.iq

1. INTRODUCTION

Due to the scarcity of fossil fuels, alternative energy sources such as renewable energy sources are becoming more appealing to researchers. Due to the low voltage ranges generated by Photovoltaic (PV) systems [1], which are renewable sources of energy are a popular topic [2], [3]. Connecting to the grid side necessitates the use of a high-efficiency boost converter [4]. The conventional boost converter is the most common type of boosting voltage [5]. This converter can only convert voltage levels in a limited range. In addition, to achieve high voltage gain in this converter, the duty cycle must be very high [6]. As a result, the power semiconductors are subjected to high voltage stress as a result of this problem [6], [7]. The source current ripple in step-up DC-DC converters should be minimal since a low source current-ripple might cause an increase in the power producer's lifetime [8]. In reality, limiting the voltage stress on the active switch and output diode if the output voltage is high is crucial, on the other hand, substantial conduction loss and high costs would result [9]. Due to parasitic properties like the inductor's internal resistance, traditional boost converters never create a high voltage [10]. A very short turn-off time will result in a huge peak current as well as significant conduction and switching losses. One of the key properties of interleaved structures is low source current ripple [11], [12]. The design given in [11] has a voltage gain that is equivalent to the typical boost converter. As a result, of high voltage gain, the duty cycle of this converter needs to greatest possible.

Although despite the fact that the source current ripple in [13] is modest, this converter is subjected to high voltage stress. The high gain topology presented in [14] suffers from high voltage stress and high source current-ripple. Increase the turn ratio of the high-frequency transformer in isolated converters to enhance the voltage ratio [15]. On the other hand, the leaking inductor must be treated with care; otherwise, voltage spikes will occur throughout the diodes or power switches [16]. Furthermore, due to multistage DC-AC-DC conversion, system size, and economy are advantages of isolated DC-DC converters [17]. A lot of coupled inductor-based high step-up converters were created, with high voltage gain achieved by increasing the coupled inductor's turn ratio to that of isolated converters [18]. Researchers [19], [20], discusses several switched-inductor and switched-capacitor structures for extending voltage gain. Introduces a novel multi-input multi-output, high voltage gain with low voltage stress is obtained in this configuration by the addition of a switched capacitor [21]-[23].

In the proposed converter high voltage gain with a wide range of duty ratio is achieved with minimal voltage stress and reduced input current ripple because of these characteristics, this structure might be a viable renewable energy converter. Because of the discontinuous flow mode's performance, main switches are automatically turned ON within zero current in the proposed converters, and the yield diodes' reverse bias issue is reduced. The auxiliary commutation circuits offer a brief if the main switch is switched OFF, the current becomes zero. Section 2 from this paper included the suggested structure and operational modes, voltage gain, source current-ripple, and voltage stresses across power semiconductors are discussed. Section 3 contains the design of considerations and the formulas in detail. In section 4, compare the performance of the proposed converter with some topology [24], [25]. Finally, in section 5 the MATLAB/Simulink program results are used to simulate and assess the suggested converter's performance.

2. THE PROPOSED CONVERTER

Figure 1 shows the proposed converter topology, which includes two inductors at the input source utilizing interleaving technical to reduce source current ripple, and two voltage multiplier units to boost output voltage. The switches are turned ON and OFF in the specified intervals. These waveforms as shown in Figure 2 are analyzed in this study as two square waves by the identical duty cycle and 180° phase difference; hence, the source current ripple and the input filter's volume might be drastically reduced. Each side of the proposed converter is a conventional converter connected in series with a voltage multiplier. Each switching capacitor-inductor circuit boosts the output voltage of one side of these converters.

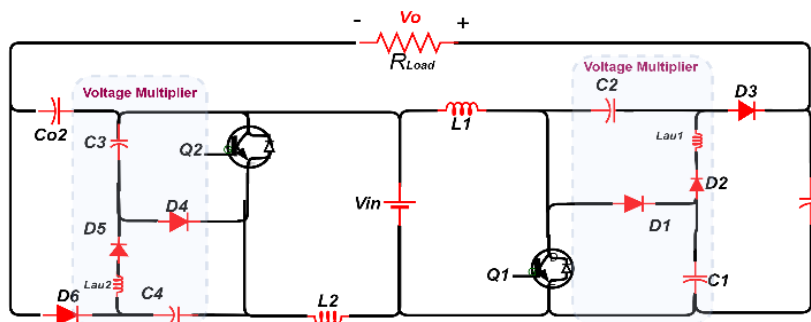


Figure 1. The proposed converter's schematic diagram

2.1. Analysis of proposed converter in steady-state

The following assumptions are assumed in this section to simplify the analysis:

- i) The proposed converter operates in continuous conduction mode (CCM).
- ii) All of the components are considered to be ideal.
- iii) The voltages of capacitors remain constant.
- iv) Input voltage is constant.
- v) The parasitic resistance of connected inductors and the ESR of capacitors are ignored.
- vi) The duty cycle is greater than 50% as shown in Figure 2
- vii) Pulse width modulation (PWM) signals control both Q1 and Q2 with a phase shift of 180 degrees as shown in Figure 2.

2.2. Circuit modes

The proposed converter operates with a high conversion ratio there for the switches Q1 and Q2 are driven by turning ON and OFF in the specified intervals with a 180°. Phase difference, and a duty cycle greater than 0.5 as shown in Figure 2.

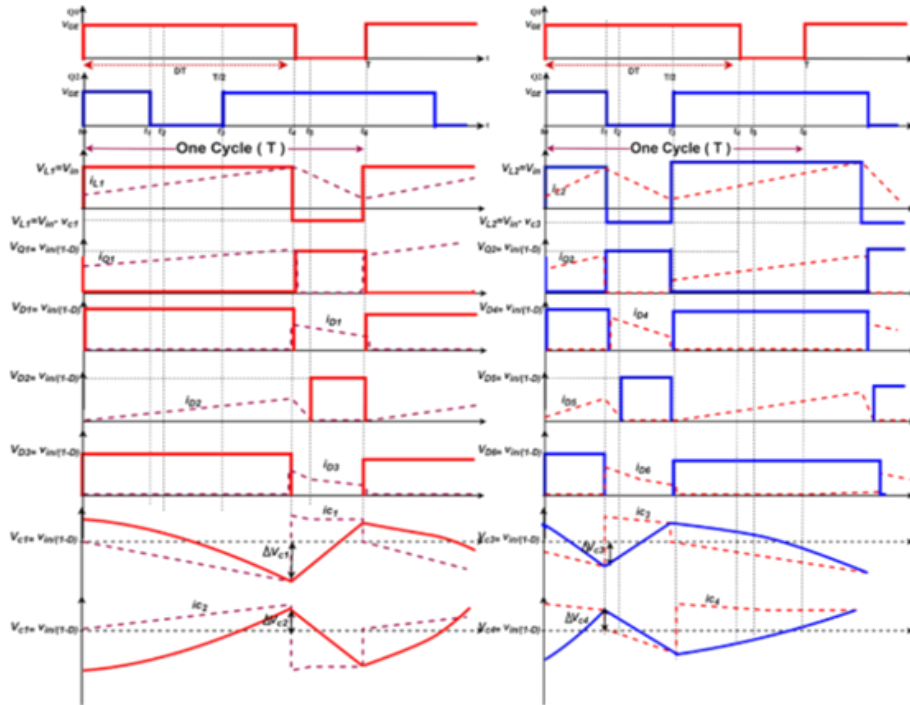


Figure 2. The proposed converter's main waveforms

Mode 1: $t_0 \leq t \leq t_1$: Duration operation in this mode is considered by $(D-0.5) T$ as shown in Figure 2. Both switches Q1 and Q2 of the proposed converter are turned ON, and the energy increases both inductors L1 and L2, where the voltage input is applied to two inductors L1 and L2. Mode 1 is indicated in Figure 3.

$$I_{L1}(t) = I_{L1}(t_0) + \frac{V_{in}}{L_1} \cdot (t - t_0) \tag{1}$$

$$I_{L2}(t) = I_{L2}(t_0) + \frac{V_{in}}{L_2} \cdot (t - t_0) \tag{2}$$

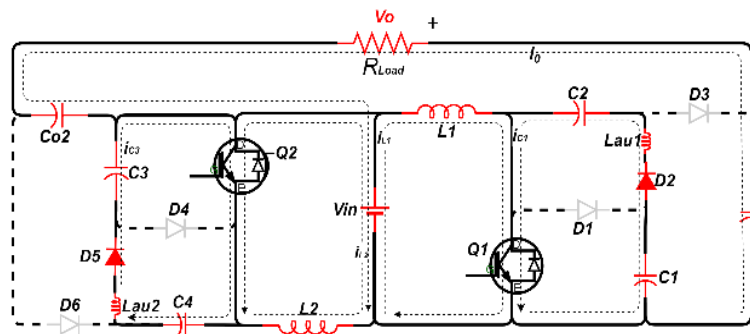


Figure 3. The proposed converter in mode 1 and mode 4

Mode 2: $t_1 \leq t \leq t_2$: Duration operation in this mode is considered by $(d) T$ as shown in Figure 2. Switch Q1 is continue turned ON and switch Q2 is turned OFF, the energy continues to increase in the inductor L1 and decreases in the inductor L2. Mode 2 is indicated in Figure 4.

$$I_{L1} = I_{L1}(t_5) + \frac{V_{in}-V_{C1}}{L_1} \cdot (t - t_5) \tag{11}$$

$$I_{L2}(t) = I_{L2}(t_5) + \frac{V_{in}}{L_2} \cdot (t - t_5) \tag{12}$$

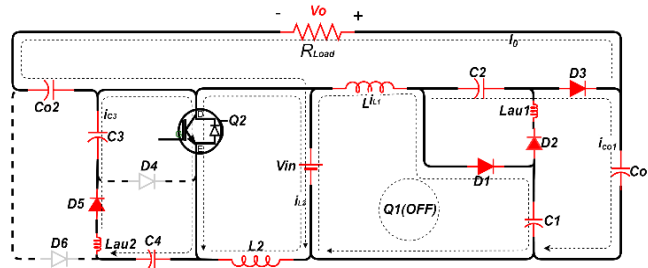


Figure 6. The proposed converter in mode 5

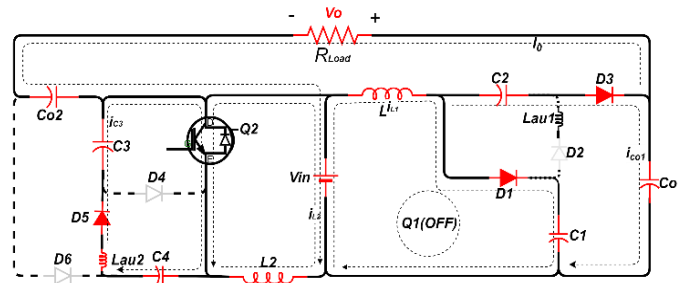


Figure 7. The proposed converter in mode 6

2.3. Voltage gain derivation

Based on the principle of the balance of the voltage second, for the inductors (L1, Lau1, L2, and Lau2), Can be calculated capacitors C1 and C2 voltages can be obtained as (13) to (15).

$$V_{C1} = \frac{V_{in}}{1-D} \tag{13}$$

$$V_{C2} = \frac{D}{d+D} \cdot V_{C1} ; d \ll D \tag{14}$$

$$V_{C1} \approx V_{C2} = \frac{V_{in}}{1-D} \tag{15}$$

The capacitors C3 and C4 voltages can be obtained as (16) to (18).

$$V_{C3} = \frac{V_{in}}{1-D} \tag{16}$$

$$V_{C4} = \frac{D}{d+D} \cdot V_{C3} ; d \ll D \tag{17}$$

$$V_{C4} \approx V_{C3} = \frac{V_{in}}{1-D} \tag{18}$$

By using Kirchhoff's voltage law in the cycle $V_{C1}-V_{C2}-V_{Co1}$, it is possible to derive the following (19) to (21).

$$V_{Co1} = V_{C1} + V_{C2} = \frac{2V_{in}}{1-D} \tag{19}$$

By using Kirchhoff's voltage law in the cycle $V_{C3}-V_{C4}-V_{Co2}$

$$V_{Co2} = V_{C3} + V_{C4} = \frac{2V_{in}}{1-D} \tag{20}$$

By using Kirchhoff's voltage law in the cycle $V_{in} - V_{CO1} - V_O - V_{CO2}$

$$\frac{V_O}{V_{in}} = \frac{3+D}{1-D} \quad (21)$$

2.4. Voltage Stress derivation

The voltage stresses for each of the main switches might be calculated as (22).

$$V_{Q1} = V_{Q2} = V_{C2} = V_{C3} = \frac{V_{in}}{1-D} \quad (22)$$

The voltage stresses across each diode are also computed as (23).

$$V_{D1} = V_{D2} = V_{D3} = V_{D4} = V_{D5} = V_{D6} = \frac{V_{in}}{1-D} \quad (23)$$

2.5. Current Ripple derivation

The input current ripple of the proposed converter can derive from the sum of the inductor current ripple in duration mode 1 as shown in Figure 2 and is decreased with increasing duty cycle at fixed level output voltage, or increasing the switching frequency.

$$\Delta I_{L1} = \Delta I_{L2} = \frac{V_{in}D}{f_s L_{1,2}} = \frac{V_O \cdot D \cdot (1-D)}{(3+D) \cdot f_s \cdot L_{1,2}}; f_s = \frac{1}{T_S}, L_1 = L_2 \quad (24)$$

$$\begin{aligned} \Delta I_{in} &= \Delta I_{L1Mode1} + \Delta I_{L2Mode1} \\ \Delta I_{in} &= \frac{V_{in}(D-0.5)}{f_s L_1} + \frac{V_{in}(D-0.5)}{f_s L_2} \end{aligned} \quad (25)$$

$$\Delta I_{in} = \frac{V_{in}(2D-1)}{f_s L}, \text{ when } L_1 = L_2 = L \quad (26)$$

3. COMPONENTS DESIGN

3.1. Inductor design

For lossless converters in (CCM) conditions operating, the output power is equal to the input power.

$$I_{inav} = \frac{V_O I_O}{V_{in}} = \frac{(3+D) \cdot I_O}{1-D} \quad (27)$$

$$I_{Lmin} = 0; I_{Lav} = \frac{I_{inav}}{2} = \frac{\Delta I_L}{2}; (\text{At boundary Condition}) \quad (28)$$

The minimum value of the inductance can be obtained as (29).

$$L_{min} \geq \frac{R_L \cdot D \cdot (1-D)^2}{f_s \cdot (3+D)^2}; \quad (29)$$

To design the inductors Lau1 and Lau2, when the main switches are turned ON, the voltage at the terminals of the auxiliary inductors can be obtained as (30) and (31).

$$V_{Lau1,2} \approx \frac{\Delta V_{C1} + \Delta V_{C2}}{2} \quad (30)$$

$$L_{au1,2} \approx \frac{V_{Lau1,2}}{f_s \cdot \Delta I_{Lau1,2}} \quad (31)$$

3.2. Capacitors design

For a period (1-D) T, the current flows through the capacitor C2 is half the average input current and the variable voltage ΔV_{C2} on its could be calculated.

$$V_{C2}(t) = \frac{1}{C_2} \int \frac{I_{inav}}{2} dt \quad (32)$$

$$V_{C2}(t) = \frac{I_{inav}}{2C_2} (t - DT) + V_{C2}(DT); DT \leq t \leq T \quad (33)$$

$$\Delta V_{C2} = V_{C2}(T) - V_{C2}(DT) = \frac{I_{inav}}{2C_2} \cdot (1 - D)T \tag{34}$$

Similarly, the capacitors $C_1, C_3,$ and C_4 have the same design (35).

$$C_1 = C_2 = C_3 = C_4 = \frac{I_{inav}}{2f_s \Delta V_C} \cdot (1 - D) \tag{35}$$

During the operating period specified in the DT period, C_{o1} and C_{o2} feed the load the necessary current.

$$\Delta V_{CO2} = \Delta V_{CO1} = \frac{I_o \cdot D}{C_o \cdot f_s} \tag{36}$$

$$\Delta V_o = 2 \cdot \frac{I_o \cdot D}{C_o \cdot f_s} \tag{37}$$

4. REVIEW OF COMPARISON

Table 1 shows the results of the comparison with the proposed converter compared to alternative topologies in terms of voltage gain, voltage stress, and current-ripple. Figure 8 compares the voltage ratio to other topologies in which the voltage gain in Figure 8(a) has been improved, and it is the best of the previous topologies. Figure 8(b) and Figure 8(c) show low voltage stress on semiconductor switches, indicating that the duty cycle can be increased to increase the voltage ratio while maintaining stress on main switches.

Table 1. A comparison of the proposed converter with other topologies

Topology	C.B converter	[21]	[13]	[25]	[24]	Prop. converter
Active switches	1	1	2	2	1	2
Diodes	1	4	3	2	4	6
Capacitor	1	1	3	3	4	6
Inductors	1	2	2	3	1	2
Voltage gain	$\frac{1}{1-D}$	$\frac{1+D}{1-D}$	$\frac{2}{1-D}$	$\frac{1+3D}{1-D}$	$\frac{3-D}{1-D}$	$\frac{3+D}{1-D}$
Voltage stress of switch	V_o	V_o	$\frac{V_o}{2}$	$\frac{V_{in}}{2}$	$\frac{V_{in}}{1-D}$	$\frac{V_{in}}{1-D}$
Voltage stress of diodes	V_o	V_o	$\frac{V_o}{2}$	$\frac{1-D}{2V_{in}}$	$\frac{1-D}{V_{in}}$	$\frac{1-D}{V_{in}}$
Current-ripple	High	High	Very low	High	High	Very low

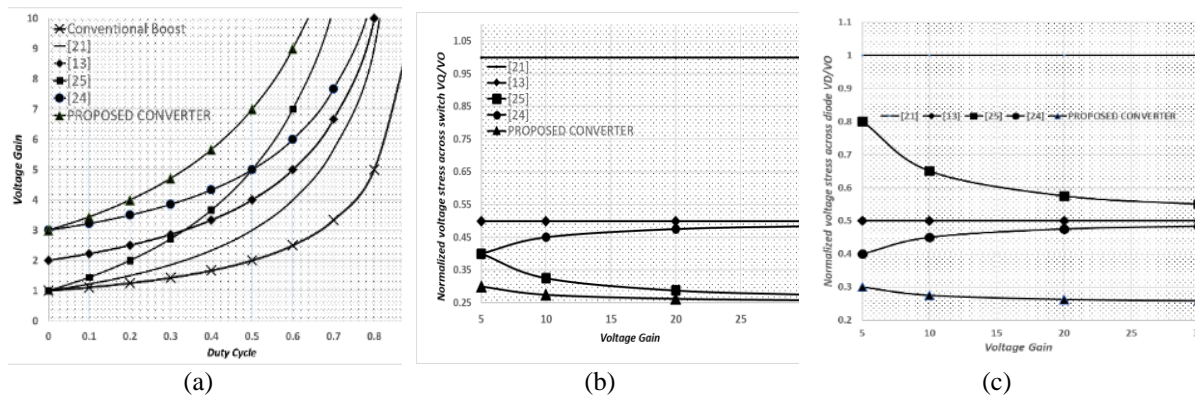


Figure 8. Comparison with other topologies (a) voltage gain as a function of the duty cycle, (b) voltage stress across the power switches, and (c) voltage stress across the power diodes

5. SIMULATION AND RESULTS

The proposed converter is simulated in MATLAB/Simulink program in this section to enhance the mathematical calculations and the characteristics of the proposed converter simulation model are listed In Table 2. Figure 9 shows the switching waveforms of the power switch Q1 and Q2, showing up the voltages' stresses on the power switches is 105 volts, which is consistent with the mathematical results. The average source current is 12 A, with a current ripple of 0.886 A. The calculated output voltage is 380 V. The output current is equal to 1.183 A.

Table 2. Component value of the proposed converter

Parameter	Value
Input voltage	38 V
Output Voltage	380 V
Duty Cycle	64%
Switching frequency	30 KHZ
Output power	450 W
Main inductors	400 μ H
Auxiliary inductors	5 μ H
Capacitors C1~ C4	25 μ F
Co1 and Co2	100 μ F

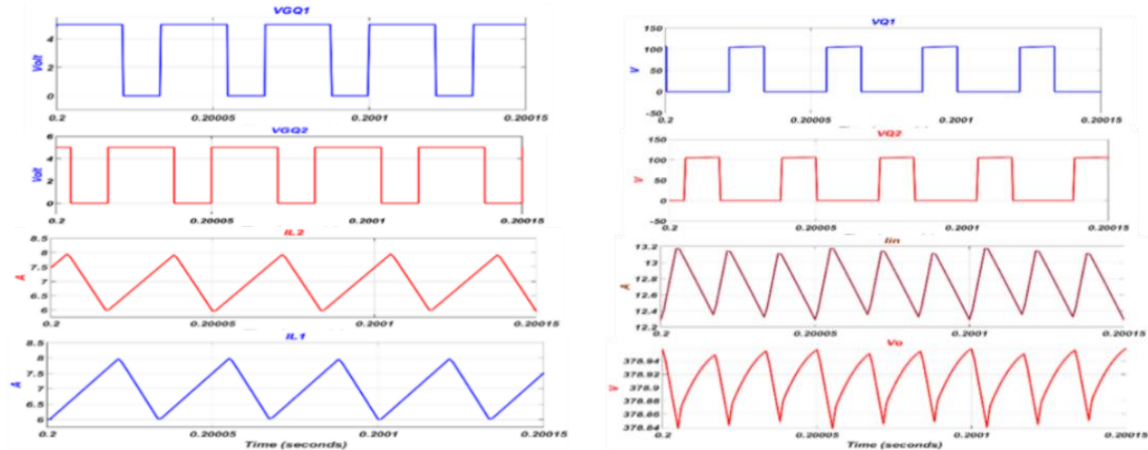


Figure 9. Simulation results voltages and currents waveform

6. CONCLUSION

A high gain DC-DC converter is provided in this paper. Two thrust converters are combined in opposite directions with the power supply, switch capacitors are connected on both sides of the output. A high voltage gain multiplier circuit is provided. Moreover, by using two inductors on both sides of the input, the ripple of the source current is decreased. For this reason, this converter can be used in renewable energy due to its qualities. Moreover, with this figure, the voltage stresses across the switches are smaller than they were previously. Some converters are mentioned for comparison in this study, to validate the mentioned requirements, and the comparison of this converter with other related converters has been completed. In addition, to prove the mathematical calculations, the MATLAB/Simulink simulation program is used.





REFERENCES

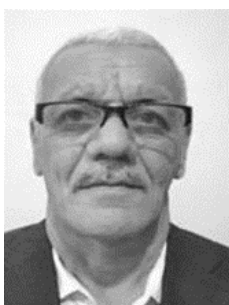
- [1] V. V. R. Scarpa, S. Buso, and G. Spiazzi, "Low-complexity MPPT technique exploiting the PV module MPP locus characterization," *IEEE transactions on industrial electronics*, vol. 56, no. 5, pp. 1531-1538, May 2009, doi: 10.1109/TIE.2008.2009618.
- [2] T. Shimizu, O. Hashimoto, and G. Kimura, "A novel high-performance utility-interactive photovoltaic inverter system," *IEEE transactions on power electronics*, vol. 18, no. 2, pp. 704-711, March 2003, doi: 10.1109/TPEL.2003.809375
- [3] E. Can, "The design and experimentation of the new cascaded DC-DC boost converter for renewable energy," *International Journal of Electronics*, vol. 106, no. 9, pp.1374-1393, 2019, doi: 10.1080/00207217.2019.1591529.
- [4] W. Li and X. He, "Review of nonisolated high-step-up DC/DC converters in photovoltaic grid-connected applications," *IEEE Transactions on Industrial Electronics*, vol. 58, no. 4, pp. 1239-1250, April 2011, doi: 10.1109/TIE.2010.2049715.
- [5] F. L. Tofoli, D. de C. Pereira, W. J. de Paula, and D. de S. O. Junior, "Survey on non-isolated high-voltage step-up dc-dc topologies based on the boost converter," *IET power Electronics*, vol. 8, no. 10, pp. 2044-2057, 2015, doi: 10.1049/iet-pel.2014.0605.
- [6] M. K. Kazmierczuk, *Pulse-width modulated DC-DC power converters*, John Wiley & Sons, 2015.
- [7] A. Thiagarajan, S. G. P. Kumar, and A. Nandini, "Analysis and comparison of conventional and interleaved DC/DC boost converter," *Second International Conference on Current Trends in Engineering and Technology - ICCTET 2014*, 2014, pp. 198-205, doi: 10.1109/ICCTET.2014.6966287.
- [8] P. Alavi, V. Marzang, E. Nazari, M. Dezhbord, and E. Babaei, "New interleaved structure with high voltage-gain and low voltage-stress on semiconductors," *2019 10th International Power Electronics, Drive Systems and Technologies Conference (PEDSTC)*, 2019, pp. 498-503, doi: 10.1109/PEDSTC.2019.8697271.
- [9] A. A. Elbaset, S. A. M. Abdelwahab, H. A. Ibrahim, and M. A. E. Eid, *Performance analysis of photovoltaic systems with energy storage systems*, Springer, 2019.





- [10] A. Sangswang and C. O. Nwankpa, "Noise characteristics of DC-DC boost converters: experimental validation and performance evaluation," *IEEE Transactions on Industrial Electronics*, vol. 51, no. 6, pp. 1297-1304, Dec. 2004, doi: 10.1109/TIE.2004.837908.
- [11] W. Li, X. Lv, Y. Deng, J. Liu, and X. He, "A review of non-isolated high step-up DC/DC converters in renewable energy applications," *2009 Twenty-Fourth Annual IEEE Applied Power Electronics Conference and Exposition*, 2009, pp. 364-369, doi: 10.1109/APEC.2009.4802683.
- [12] L.-S. Yang, T.-J. Liang, and J.-F. Chen, "Transformerless DC-DC converters with high step-up voltage gain," *IEEE Transactions on Industrial Electronics*, vol. 56, no. 8, pp. 3144-3152, 2009, doi: 10.1109/TIE.2009.2022512.
- [13] P. Wang, L. Zhou, Y. Zhang, J. Li, and M. Sumner, "Input-parallel output-series DC-DC boost converter with a wide input voltage range, for fuel cell vehicles," *IEEE Transactions on Vehicular Technology*, vol. 66, no. 9, pp. 7771-7781, 2017, doi: 10.1109/TVT.2017.2688324.
- [14] Y. Tang, T. Wang, and Y. He, "A switched-capacitor-based active-network converter with high voltage gain," *IEEE transactions on power electronics*, vol. 29, no. 6, pp. 2959-2968, June 2014, doi: 10.1109/TPEL.2013.2272639.
- [15] S. JemeJemei, D. Hissel, M.-Cé. PÉraPera, and J. M. Kauffmann, "A new modeling approach of embedded fuel-cell power generators based on artificial neural network," *IEEE Transactions on Industrial Electronics*, vol. 55, no. 1, pp. 437-447, Jan. 2008, doi: 10.1109/TIE.2007.896480.
- [16] V. S. Nayagam and L. Premalatha, "Green energy based coupled inductor interleaved converter with MPPT technique for BLDC application," *International Journal of Power Electronics and Drive Systems*, vol. 9, no. 4, p. 1725, 2018. doi: 10.11591/ijpeds.v9.i4.pp1725-1732.
- [17] B. Rajapandian and G. T. Sundarajan, "Evaluation of DC-DC converter using renewable energy sources," *International Journal of Power Electronics and Drive Systems*, vol. 11, no. 4, p. 1918, 2020, doi: 10.11591/ijpeds.v11.i4.pp1918-1925.
- [18] C.-M. Wang, "A novel ZCS-PWM flyback converter with a simple ZCS-PWM commutation cell," *IEEE Transactions on Industrial Electronics*, vol. 55, no. 2, pp. 749-757, 2008, doi: 10.1109/TIE.2007.911917.
- [19] F. Forest, T. A. Meynard, E. Labouré, B. Gelis, J.-J. Huselstein, and J. C. Brandelero, "An isolated multicell intercell transformer converter for applications with a high step-up ratio," *IEEE transactions on power electronics*, vol. 28, no. 3, pp. 1107-1119, 2012, doi: 10.1109/TPEL.2012.2209679.
- [20] L. Zhou, B. Zhu, Q. Luo, and S. Chen, "Interleaved non-isolated high step-up DC/DC converter based on the diode-capacitor multiplier," *IET Power Electronics*, vol. 7, no. 2, pp. 390-397, 2014, doi: 10.1049/iet-pel.2013.0124.
- [21] B. Axelrod, Y. Berkovich, and A. Ioinovici, "Switched-capacitor/switched-inductor structures for getting transformerless hybrid DC-DC PWM converters," *IEEE Transactions on Circuits and Systems I: Regular Papers*, vol. 55, no. 2, pp. 687-696, 2008, doi: 10.1109/TCSI.2008.916403.
- [22] M. Prudente, L. L. Pfitscher, G. Emmendoerfer, E. F. Romaneli, and R. Gules, "Voltage multiplier cells applied to non-isolated DC-DC converters," *IEEE Transactions on Power Electronics*, vol. 23, no. 2, pp. 871-887, 2008, doi: 10.1109/TPEL.2007.915762.
- [23] K.-C. Tseng, C.-C. Huang, and W.-Y. Shih, "A high step-up converter with a voltage multiplier module for a photovoltaic system," *IEEE transactions on power electronics*, vol. 28, no. 6, pp. 3047-3057, 2012, doi: 10.1109/TPEL.2012.2217157.
- [24] B. Wu, S. Li, Y. Liu, and K. M. Smedley, "A new hybrid boosting converter for renewable energy applications," *IEEE Transactions on Power Electronics*, vol. 31, no. 2, pp. 1203-1215, 2015, doi: 10.1109/TPEL.2015.2420994.
- [25] M. A. Salvador, T. B. Lazzarin, and R. F. Coelho, "High step-up DC-DC converter with active switched-inductor and passive switched-capacitor networks," *IEEE Transactions on Industrial Electronics*, vol. 65, no. 7, pp. 5644-5654, 2017, doi: 10.1109/TIE.2017.2782239.

BIOGRAPHIES OF AUTHORS



Ibraheem Jawad Billy     is a Master's Student at the College of Electrical Engineering, University of Technology & Baghdad, Iraq. He received a B.Sc. in Electrical Engineering from the University of Babylon, Iraq in 2006. He is currently working toward an M. Sc degree in Electrical Engineering at the University of Technology, Iraq. His research interest is in the area of DC-DC converters, controller design, and renewable energy. He can be contacted at email: eee.20.28@grad.uotechnology.edu.iq.



Dr. Jasim Farhood Hussein     received the B.Sc. in Electrical Science from the University of Technology Iraq-Baghdad in 1989 and 2003 respectively, and the Ph.D. degree in Electrical Engineering from The Montfort University, U.K. His area of interest includes of power electronics field and renewable energy. He can be contacted at email: 3705@uotechnology.edu.iq.